Finite difference time domain simulations of dynamic materials to inform warm dense matter experiments

Jack Roth

(Dated: 24 August 2018)

Measuring the DC conductivity of warm dense matter (WDM) is of general interest as it will inform models of a variety of astrophysical and planetary phenomena, including the production of the currents at the Earth's core responsible for Earth's magnetic field. Low frequency conductivity measurements can be performed via terahertz spectroscopy, in which a terahertz laser pulse is transmitted through WDM. The transmitted pulse can be used to determine the complex conductivity of the WDM as a function of frequency. However, given that WDM states are unstable and evolve in their phase space on timescales shorter than that of the terahertz pulse, it is important to investigate the affect that this evolution has on the transmitted pulse. Recursive convolution finite difference time domain (RC-FDTD) simulations can be used to investigate this affect in conventional materials, with the hope that any insights will generalize to WDM experiments. Preliminary results of this simulation technique are explored.

I. INTRODUCTION

When solid matter is heated into a plasma on a short timescale the heated matter briefly passes through a state of matter known as warm dense matter (WDM). As the matter is heated on such a short timescale the heating occurs isochorically, meaning that the matter, despite having the temperature of a typical plasma, is confined within the volume of its solid phase state. Without the enormous pressures required to contain the WDM within its original volume, the WDM state is rendered unstable and quickly expands, exiting the WDM phase and entering a plasma phase. Recently it has become possible to investigate such WDM states in the laboratory.

Stable WDM states exist in systems under extreme pressure, such as planetary cores, white dwarfs, and brown dwarfs. WDM at the Earth's core is responsible producing Earth's magnetic field. Characterizing the DC electrical conductivity (referred to hereafter as conductivity) of WDM states is of interest because, amongst other reasons, it could lead to a deeper understanding of how Earth's magnetic fields are generated.

The low frequency behavior of conductivity in WDM states can be examined through terahertz spectroscopy. In these experiments a terahertz pulse is transmitted through a sample. The pulse amplitude can be sampled in time, yielding a time profile of the transmitted pulse. This transmission can, in the thin sample limit[6], yield a measurement of the complex conductivity of the sample. As terahertz pulses are composed of low frequencies (rather than in infrared frequencies or higher) near DC conductivity can be determined via this method.

Terahertz pulses last for timescales of around 500fs. Due to the unstable nature of laboratory induced WDM states, it cannot be assumed that WDM conductivity is constant over a 500fs timescale. Therefore it is of interest to determine how matter changing on the timescale of a terahertz pulse affects the conductivity measurement extracted from that pulse. Due to the difficulty of accurately modeling WDM, we have chosen to investigate this same problem in conventional materials. The remainder of this paper describes a simulation method and how that simulation method can determine how changing material conductivity effects a terahertz conductivity measurement of that material.

II. RC-FDTD

Recursive convolution finite difference time domain (RC-FDTD) simulations have long been used to numerically solve Maxwell's equations. This simulation technique discretizes the time domain and evolves the electric and magnetic fields in time using a set of update equations. Within the simulation, space is discretized into intervals of length Δz and time into intervals of length Δt. A specific point in time and space is accessed via $z = i\Delta z$ and $t = n\Delta t$. The simulation relies on a number of assumptions:

- All materials are linear dielectrics such that $P(z,\omega) = \epsilon_0 \chi E(z,\omega)$.
- The electric and magnetic fields are plane waves propagating along spatial coordinate z.
- Materials are uniform along spatial coordinates x and y.
- The electric and magnetic fields are zero for all time prior to the start of the simulation ($E(z,t) = 0$ for all $t < 0$).
- The electric field $E(z,t)$ is approximately constant over all time intervals of duration Δt.
- The magnetization of all materials is zero ($\vec{M} = \vec{0}$).

These assumptions allow the derivation of the discretized displacement field $D^{i,n}$

$$D^{i,n} = \epsilon_0 \epsilon_\infty E^{i,n} + \epsilon_0 \sum_{m=0}^{n-1} E^{i,n-m} \chi^m$$

where

$$\chi^m = \int_{m\Delta t}^{(m+1)\Delta t} \chi(\tau) \mathrm{d}\tau \tag{1}$$

This result is derived in appendix A, and is crucial for the subsequent derivation of the electric and magnetic field update equations[1,3] derived in appendix B and given below

$$H^{i+1/2,n+1/2} = H^{i+1/2,n-1/2} - \frac{1}{\mu_0}\frac{\Delta t}{\Delta z}\left[E^{i+1,n} - E^{i,n}\right] \tag{2}$$

$$\begin{aligned} E^{i,n+1} =& \frac{\epsilon_\infty}{\epsilon_\infty + \chi^0} E^{i,n} + \frac{1}{\epsilon_\infty + \chi^0}\psi^n - \frac{\Delta t I_f}{\epsilon_0\left[\epsilon_\infty + \chi^0\right]} \\ & - \frac{1}{\epsilon_0\left[\epsilon_\infty + \chi^0\right]}\frac{\Delta t}{\Delta z}\left[H^{i+1/2,n+1/2} - H^{i-1/2,n+1/2}\right] \end{aligned} \tag{3}$$

where

$$\begin{aligned} \Delta\chi^m &= \chi^m - \chi^{m+1} \\ \psi^n &= \sum_{m=0}^{n-1} E^{i,n-m}\Delta\chi^m \end{aligned} \tag{4}$$

The accuracy of the derivative approximation inherent to these update equations relies on choosing some Δz and Δt small enough such that the electric and magnetic fields are approximately linear over spatial intervals Δz and time intervals Δt. If this condition is not met then the accuracy of the derivative approximation breaks down. The update equations derived here are significant as they reveal that any linear dielectric can be accurately simulated via the RC-FDTD method as long as the electric susceptibility of the material $\chi(t)$ is well defined. We turn our attention to modeling the electric susceptibility of materials in section III.

III. MODELING ELECTRIC SUSCEPTIBILITY

We implement a model for the electric susceptibility of a material that considers the classical interaction between an electron and an atomic nucleus of the same charge[1,2]. The net force on the electron can be described as follows

$$\underbrace{m_e\ddot{x}(t)}_{F=ma} = \underbrace{q_e E(t)}_{\text{driving force}} - \underbrace{2m_e\gamma\dot{x}(t)}_{\text{damping force}} - \underbrace{m_e\omega_0^2 x(t)}_{\text{restoring force}} \tag{5}$$

where γ is the damping constant, ω_0 is the natural frequency of the oscillator, and $E(t)$ is the electric field along the displacement axis. The general solution of this differential equation is well known

$$x(t) = e^{-\gamma t}\left[A_1' e^{\beta t} + A_2' e^{-\beta t}\right]$$

where $\beta = \sqrt{\gamma^2 - \omega_0^2}$. In order to model the electric susceptibility resulting from an arbitrary periodic driving electric field we allow a linear combination of solutions $x_j(t)$ indexed by j. This allows the modeling of any arbitrary periodic driving electric field[9].

The time displacement of a single oscillating electron is used to determine the electric susceptibility $\chi(t)$ of a simulated material. Consider the dipole moment produced by the electron-atomic nucleus charge pair $p(t) = q_e x(t)$. Letting N such electron-atomic nucleus oscillators exist per unit volume of the material, it is found that the polarization per unit volume of the material is $P(t) = Np(t) = Nq_e x(t)$. Since $\chi(\omega)E(\omega) = P(\omega)$, $P(t)$, $\chi(t)$, and $E(t)$ are related via the convolution

$$\int_{-\infty}^{t} \chi(\tau)E(t-\tau)\mathrm{d}\tau = P(t) = Nq_e x(t)$$

Thus in the presence of a dirac delta function electric field the electric susceptibility of the material is[1]

$$\chi(t) = \sum_j e^{-\gamma_j t}\left[A_{j,1}e^{\beta_j t} + A_{j,2}e^{-\beta_j t}\right] \tag{6}$$

where Nq_e is absorbed into $A'_{j,1}$ and $A'_{j,2}$ to get $A_{j,1}$ and $A_{j,2}$. This result can be combined with Eq.(1) to yield a computationally efficient update equation for Eq.(4), discussed in Beard et al.. Via a Fourier transform of Eq.(5) and noting that $\chi(\omega)E(\omega) = P(\omega) = Nq_e x(\omega)$ we find the electric susceptibility of the material in the frequency domain to be

$$\chi(\omega) = \frac{Nq_e^2/m_e}{\omega_0^2 - \omega^2 + 2i\gamma\omega} \tag{7}$$

IV. STATIC AND DYNAMIC MATERIALS

Often materials investigated via a spectroscopic measurement are in thermodynamic equilibrium. We will call these materials *static materials* as they are static within their respective phase spaces[4]. In order to demonstrate the ability of the model derived in section III to describe a static material we show how this general model can be reduced to the Drude model. For a lossy material where $\epsilon_r = 1$

$$\chi(\omega) = -\frac{i\sigma(\omega)}{\omega} \rightarrow \sigma(\omega) = i\omega\chi(\omega)$$

Drude metals have no restoring force, meaning $\omega_0 = 0$. Using Eq.(7) as a definition for $\chi(\omega)$

$$\sigma(\omega) = \frac{1}{2\gamma} \frac{Nq_e^2/m_e}{1 - \frac{\omega}{2i\gamma}}$$

Let $\tau = \frac{1}{2\gamma}$ and $\sigma_0 = Nq_e^2\tau/m_e$

$$\sigma(\omega) = \frac{\sigma_0}{1 + i\omega\tau} \tag{8}$$

which is known to be the conductivity of a Drude metal[6]. Thus by selecting $A_1 = -A_2$ and $\beta = \gamma$ for all j, Eq.(6) reduces from our general electric susceptibility to the electric susceptibility of a Drude metal. A simulation of a Drude metal is performed in section V, and serves as a test of the simulation's accuracy.

Discussion so far has been limited to the case of static materials. If a material is not in thermodynamic equilibrium the definition for electric susceptibility given in Eq.(6) becomes insufficient as the parameters $A_{j,1}$, $A_{j,2}$, γ_j, and β_j acquire some time dependence. We denote such materials *dynamic materials*. The question now becomes how does one accurately model the electric susceptibility of a dynamic material within the framework of an RC-FDTD simulation.

One method of simulating dynamic materials is to define two electric susceptibility models in a single material: the excited state electric susceptibility and the ground state electric susceptibility. Both susceptibilities result from populations of excited and ground state electron-atomic nucleus oscillators discussed in section III. By varying these populations in time the material becomes dynamic[1]. This evolving electric susceptibility is given by

$$\chi(t) = f_e\chi_e(t) + (1 - f_e)\chi_g(t)$$

where f_e is the fraction of oscillators in the excited state at any point in time. In order to model f_e one is required to consider the mechanism through which oscillators are excited.

Typically some material will be excited by a visual pulse which has a gaussian profile in time with FWHM of Γ. The number of oscillators excited from their ground state at any given instant in time due to the visual pulse is proportional to the amplitude of the visual pulse at that time. Thus the fraction of oscillators moved from their ground state to their excited state at some point in time is given by the error function scaled to range $[0, 1]$.

The population of excited oscillators will experience an exponential decay in time with associated time constant τ_0. If $\Gamma \ll \tau_0$ the exponential decay begins at approximately the same time for each oscillator population excited by the visible pulse. If this assumption cannot be made then care must be taken to ensure that each excited oscillator starts to decay at the time it is initially excited.

The spatial extent of the material is a relevant consideration when formulating f_e. The visual pulse arrives at different points in the material at different times, meaning that the visual pulse amplitude is determined by both its space and time coordinates. Thus f_e is defined as

$$\begin{aligned} f_e(z,t,\Delta t) =& \frac{1}{2}\left(\mathrm{erf}_t\left[\frac{(t-t_0) - (z-z_0)/v - \Delta t}{\Gamma}\right] + 1\right) \\ & \times \exp\left[-\frac{(t-t_0) - (z-z_0)/v - \Delta t}{\tau_0}\right]\theta(t-t_0)\theta(z-z_0) \end{aligned}$$

where $\theta(\xi)$ is the Heaviside step function, t_0 is the time at which the visible pulse enters the material, z_0 is the starting location of the material, v is the speed of the visual pulse in the material, Δt is the time delay between the visual and terahertz pulse ($\Delta t < 0$ corresponds to a visual pulse that occurs before the terahertz pulse), and the error function is determined by integrating a gaussian with respect to time. The Heaviside step functions ensure that $f_e(z,t)$ is zero for times where the the visual pulse is not yet inside the material and for locations outside of the material[5].

It is relevant to note that this definition of $f_e(z,t,\Delta t)$ has two important properties

$$\lim_{t\to-\infty} f(z,t,\Delta t) = 0 \qquad \lim_{t\to\infty} f(z,t,\Delta t) = 0$$

These two properties are necessary as at times far from the presence of the visual pulse the fraction of excited oscillators should go to zero.

V. SIMULATIONS

In order to determine if the simulation could produce accurate results the Drude metal described in section IV was placed into the simulation and its conductivity was probed. Specific values of the constants present in Eq.(6) used in the simulation can be found in table I. The analytic form for the conductivity of a Drude metal given in Eq.(8) is fit to the simulated conductivity by allowing σ_0 to vary. The simulated sample is 50nm thick, much

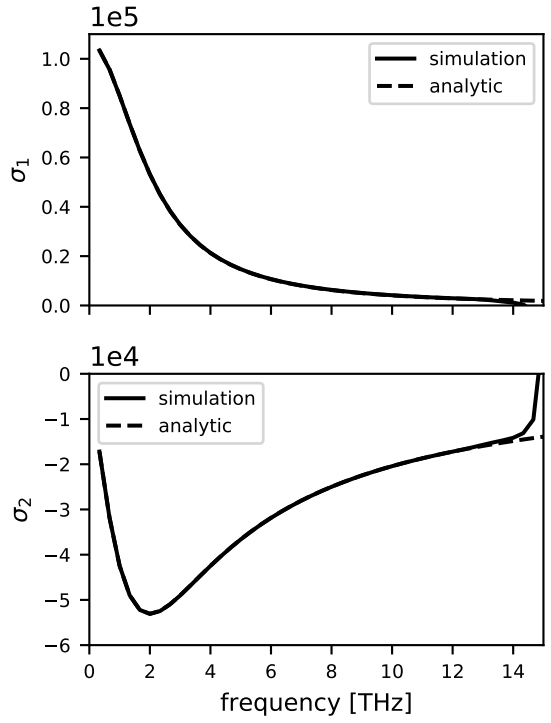

FIG. 1. The simulated and analytic conductivities of a Drude metal. σ_1 corresponds to the real part of some complex conductivity σ while σ_2 corresponds to the imaginary part. One might note that that the simulated and analytic results start to diverge around 12.5THz. This is a result of the terahertz pulse having approximately zero amplitude in frequency space beyond 12.5THz.

TABLE I. Drude metal simulation parameters.

ϵ_∞	1.000
$A_1, -A_2$	1.000×10^{16}
τ	500.0fs
γ	1.000THz

shorter than the wavelengths composing the terahertz pulse. In this limit the conductivity is given by

$$\sigma(\omega) = \frac{2}{Z_0 d}\left(\frac{1}{t(\omega)} - 1\right)$$

where Z_0 is the impedance of free space, d is the width of the sample, and $t(\omega)$ is the ratio of the transmitted terahertz pulse to the reference terahertz pulse. The the simulated and analytic forms of conductivity are nearly identical, as seen in Fig.(1).

A simulation using the dynamic material model described in section IV was performed, again on a material 50nm thick. The dynamic material in question is a Drude metal in both its ground and excited states. However, the scattering time τ of the ground and excited state differs.

TABLE II. Short visual pulse method simulation parameters

ϵ_∞	1.000
$A_{e,1}, -A_{e,2}$	1.000×10^{16}
$A_{g,1}, -A_{g,2}$	1.000×10^{16}
γ_e	10.00GHz
γ_g	1.000THz
Γ	100.0fs
τ_0	1.000ps
τ_e	50.00ps
τ_g	500.0fs

The parameters used in the simulation can be found in table II. The simulation is still in its early stages, and as such was not fit to any experimental results. The transmitted electric field $E_t(t)$ in time can be found versus the the time delay between the visual and terahertz pulse Δt in Fig.(2). The lineout plot at the bottom of Fig.(2) reveals that $E_t(t)$ is transformed by the visual pulse in a different manner depending on the value of Δt. Further analysis will reveal if this transformation is negligible, or if it significantly effects the measured conductivity of the dynamic material.

VI. CONCLUSION

We have implemented an RC-FDTD simulation and shown its ability to replicate the behavior of traditional materials, such as the Drude metal. A model for the behavior of a dynamic material has been proposed and a preliminary simulation has been performed.

There are a number of clear future directions to take this simulation method. Future simulations might use the dynamic material model proposed in section IV but simulate a material that undergoes a more drastic transition, from an insulator to a Drude metal, for example. Such simulations could reveal behavior very different from that of the dynamic simulation performed in section V. It is also of interest to propose another model for the fraction of excited oscillators f_e. Such a model might take the fact that oscillators are excited at different times and therefore have a different decay associated with them into account. Or it might account for the fact that excited oscillators emit photons through spontaneous emission that might result in the excitation of other oscillators. It is also relevant to consider the interaction between the visual pulse and the electric susceptibility at the frequency of the visual pulse, which might add a $\chi(t)_{\text{visual}}$ to the definition of $\chi(t)$[1]. It is also of interest to perform further analysis on dynamic material simulations that will reveal how conductivity measurements are effected by evolving material properties.

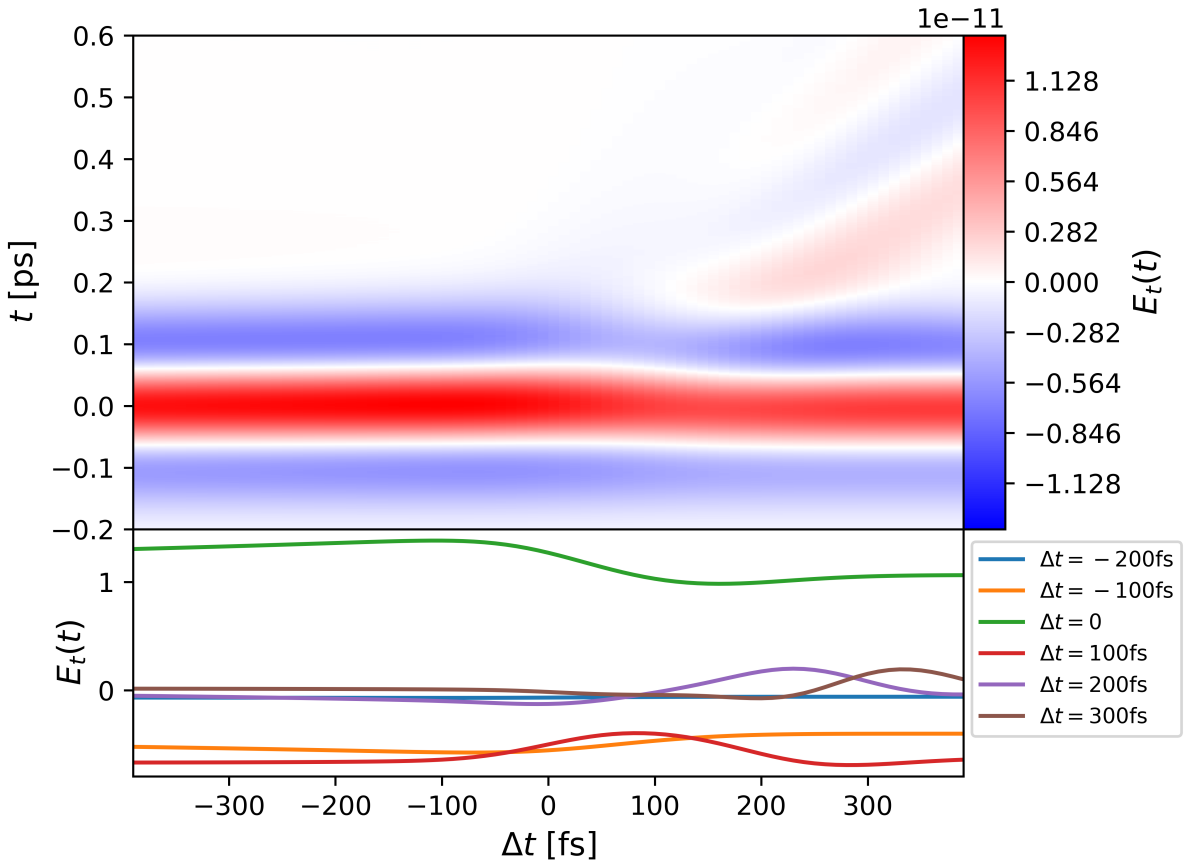

FIG. 2. The electric field transmitted through a dynamic material. The heatmap displays the amplitude of the transmitted electric field $E_t(t)$ in time and as a function of the delay Δt between the visual and terahertz pulses. The lineout plot displays the amplitude of the electric field $E_t(t)$ at specific times as a function of Δt.

VII. ACKNOWLEDGEMENTS

I would like to thank Professor Siegfried Glenzer for welcoming me into the High Energy Density Science (HEDS) research group and for providing me with crucial feedback on my presentation skills, which I am certain has pushed me to become a much more effective science communicator. In addition I would like to thank the entire HEDS group for serving as wonderful role models and mentors. Finally I would like to acknowledge the instruction I received from Benjamin Ofori-Okai in developing my understanding of the terahertz spectroscopy problem at hand and the RC-FDTD simulation technique. I would like to further thank Benjamin for his excellent mentorship and advice over the course of my internship at SLAC and hopefully beyond.

My internship was made possible by the Department of Energy SULI program. Funding was provided by the US Department of Energy under DOE Contract DE-AC02-76SF00515.

Appendix A: Deriving and discretizing the time domain displacement field

Recall the displacement field $\vec{D}(\vec{r},\omega)$ from Eq.(4.21) in Griffiths. With the requirement that simulated materials are linear dielectrics such that $P(z,\omega) = \epsilon_0\chi(z,\omega)E(z,\omega)$ and the requirement that the field varies over only the spatial coordinate z we find that $D(z,\omega)$ is

$$D(z,\omega) = \epsilon_0 \left[1 + \chi(z,\omega)\right] E(z,\omega)$$

The displacement field $D(z,\omega)$ can be transformed to the time domain via

$$\begin{aligned} D(z,t) =& \mathcal{F}^{-1}\left\{D(z,\omega)\right\} \\ =& \mathcal{F}^{-1}\left\{\epsilon_0\left[1+\chi(\omega)\right]E(z,\omega)\right\} \\ =& \mathcal{F}^{-1}\left\{\epsilon_0 \mathcal{F}\left\{1+\chi(t)\right\}\mathcal{F}\left\{E(z,t)\right\}\right\} \end{aligned}$$

where $\mathcal{F}\left\{a(t)\right\}$ and $\mathcal{F}^{-1}\left\{a(\nu)\right\}$ to denote Fourier and inverse Fourier transforms. Thus via the convolution

theorem[7]

$$\begin{aligned} D(z,t) &= \mathcal{F}^{-1}\left\{\epsilon_0 \mathcal{F}\left\{1+\chi(t)\right\}\mathcal{F}\left\{E(z,t)\right\}\right\} \\ &= \epsilon_0\left[1+\chi(t)\right] * \left[E(z,t)\right] \\ &= \epsilon_0\left[\epsilon_\infty E(z,t) + \int_0^t \chi(\tau)E(z,t-\tau)\mathrm{d}\tau\right] \end{aligned}$$

where $*$ denotes a convolution. It is assumed that $E(z,t) = 0$ for all $t < 0$. We discretize this result by replacing the z and t coordinates via $z = i\Delta z$ and $t = n\Delta t$ where $i, n \in \mathbb{R}$, yielding

$$\begin{aligned} D(i\Delta z, n\Delta t) =& \epsilon_0\epsilon_\infty E(i\Delta z, n\Delta t) \\ &+ \epsilon_0 \int_0^{n\Delta t} \chi(\tau)E(i\Delta z, n\Delta - \tau)\mathrm{d}\tau \end{aligned}$$

Assuming that $E(i\Delta z, n\Delta - \tau)$ is constant over all time intervals of duration Δt the integral is replaced with a sum

$$D^{i,n} = \epsilon_0\epsilon_\infty E^{i,n} + \epsilon_0 \sum_{m=0}^{n-1} E^{i,n-m}\chi^m \tag{A1}$$

where

$$\chi^m = \int_{m\Delta t}^{(m+1)\Delta t} \chi(\tau)\mathrm{d}\tau$$

It is *not* assumed $\chi(t)$ is constant over any time interval. This result is consistent with the result derived in Luebbers et al. and Beard et al..

Appendix B: Discretizing Maxwell's Equations

With the requirement that $\vec{M} = \vec{0}$ and the requirement that the electric and magnetic fields are uniform in spatial coordinates x and y, Faraday's law of induction and Ampere's law with Maxwell's addition reduce to

$$\frac{\partial E}{\partial z} = -\mu_0\frac{\partial H}{\partial t} \qquad -\frac{\partial H}{\partial z} = I_f + \frac{\partial D}{\partial t}$$

where I_f is along $\hat{z}$. Noting the definition of a derivative[8] we find

$$\begin{aligned} \lim_{\Delta z\to 0}\frac{E(z+\Delta z,t)-E(z,t)}{\Delta z} &= -\mu_0 \lim_{\Delta t\to 0}\frac{H(z,t+\Delta t)-H(z,t)}{\Delta t} \\ -\lim_{\Delta z\to 0}\frac{H(z+\Delta z,t)-H(z,t)}{\Delta z} &= I_f + \lim_{\Delta t\to 0}\frac{D(z,t+\Delta t)-D(z,t)}{\Delta t} \end{aligned}$$

From here the discretization process is simple. We simply remove each limit from the equations, define an appropriate value of Δz and Δt, and replace the fields with their discretized forms.

$$\frac{E^{i+1,n}-E^{i,n}}{\Delta z} = -\mu_0\frac{H^{i,n+1}-H^{i,n}}{\Delta t} \tag{B1}$$

$$-\frac{H^{i+1,n}-H^{i,n}}{\Delta z} = I_f + \frac{D^{i,n+1}-D^{i,n}}{\Delta t} \tag{B2}$$

If Δz and Δt aren't small enough such that the derivative is accurate then the RC-FDTD simulation will break down.

We solve Eq.(B1) for $H^{i,n+1}$, finding the following update equation

$$H^{i,n+1} = H^{i,n} - \frac{1}{\mu_0}\frac{\Delta t}{\Delta z}\left[E^{i+1,n} - E^{i,n}\right]$$

In order to solve Eq.(B2) we use the result of Eq.(A1) to determine $D^{i,n+1} - D^{i,n}$ in terms of $E^{i+1,n}$ and $E^{i,n}$

$$\begin{aligned} D^{i,n+1} - D^{i,n} &= \epsilon_0\epsilon_\infty E^{i,n+1} + \epsilon_0\sum_{m=0}^{n} E^{i,n+1-m}\chi^m - \epsilon_0\epsilon_\infty E^{i,n} - \epsilon_0\sum_{m=0}^{n-1} E^{i,n-m}\chi^m \\ &= \epsilon_0\epsilon_\infty\left[E^{i,n+1} - E^{i,n}\right] + \epsilon_0\left[\sum_{m=0}^{n} E^{i,n+1-m}\chi^m - \sum_{m=0}^{n-1} E^{i,n-m}\chi^m\right] \end{aligned}$$

Noting that

$$\begin{aligned}\sum_{m=0}^{n} E^{i,n+1-m}\chi^m - \sum_{m=0}^{n-1} E^{i,n-m}\chi^m &= E^{i,n+1}\chi^0 + \sum_{m=1}^{n} E^{i,n+1-m}\chi^m - \sum_{m=0}^{n-1} E^{i,n-m}\chi^m \\ &= E^{i,n+1}\chi^0 + \sum_{m=0}^{n-1} E^{i,n+1-(m+1)}\chi^{m+1} - \sum_{m=0}^{n-1} E^{i,n-m}\chi^m \\ &= E^{i,n+1}\chi^0 + \sum_{m=0}^{n-1} E^{i,n-m}\left[\chi^{m+1} - \chi^m\right]\end{aligned}$$

and letting

$$\begin{aligned}\Delta\chi^m &= \chi^m - \chi^{m+1} \\ \psi^n &= \sum_{m=0}^{n-1} E^{i,n-m}\Delta\chi^m\end{aligned}$$

we find

$$\begin{aligned}D^{i,n+1} - D^{i,n} &= \epsilon_0\epsilon_\infty\left[E^{i,n+1} - E^{i,n}\right] + \epsilon_0\left[E^{i,n+1}\chi^0 - \psi^n\right] \\ &= \epsilon_0\left[\epsilon_\infty + \chi^0\right]E^{i,n+1} - \epsilon_0\epsilon_\infty E^{i,n} - \epsilon_0\psi^n\end{aligned}$$

Substituting this result into Eq.(B2) and solving for $E^{i,n+1}$ we find

$$\begin{aligned}E^{i,n+1} =& \frac{\epsilon_\infty}{\epsilon_\infty + \chi^0}E^{i,n} + \frac{1}{\epsilon_\infty + \chi^0}\psi^n - \frac{\Delta t I_f}{\epsilon_0\left[\epsilon_\infty + \chi^0\right]} \\ &- \frac{1}{\epsilon_0\left[\epsilon_\infty + \chi^0\right]}\frac{\Delta t}{\Delta z}\left[H^{i+1,n} - H^{i,n}\right]\end{aligned}$$

We then implement the Yee cell in the simulation by offsetting the electric and magnetic field cells by half a spatial and temporal increment[1], producing the update equations Eq.(2) and Eq.(3) in section II. The derivation performed here was checked against Luebbers et al. and Beard et al. and is consistent with those two results.

REFERENCES

[1]Matthew C. Beard and Charles A. Schmuttenmaer. Using the finite-difference time-domain pulse propagation method to simulate time-resolved thz experiments. *The Journal of Chemical Physics*, 114(7):2903–2909, 2001.

[2]David J Griffiths. *Introduction to electrodynamics; 4th ed.* Pearson, Boston, MA, 2013. Re-published by Cambridge University Press in 2017.

[3]R. J. Luebbers, F. Hunsberger, and K. S. Kunz. A frequency-dependent finite-difference time-domain formulation for transient propagation in plasma. *IEEE Transactions on Antennas and Propagation*, 39(1):29–34, Jan 1991.

[4]The term static was also used in reference[1].

[5]One might take issue with the fact that there is no Heaviside step function to catch the case in which $f_e(z,t)$ is calculated at a location and time at which the visual

pulse has not reached. For such cases the error function returns a sufficiently low value that it acts as the Heaviside step function in place of an explicit one.

[6]Benjamin Kwasi Ofori-Okai. *Developments and applications of THz polaritonics, efficient THz generation, and single-shot THz detection*. PhD thesis, Massachusetts Institute of Technology, 10 2016.

[7]Eric W. Weisstein. Convolution theorem. From MathWorld—A Wolfram Web Resource. `http://mathworld.wolfram.com/ConvolutionTheorem.html`.

[8]Eric W. Weisstein. Derivative. From MathWorld—A Wolfram Web Resource. `http://mathworld.wolfram.com/Derivative.html`.

[9]Eric W. Weisstein. Fourier series. From MathWorld—A Wolfram Web Resource. `http://mathworld.wolfram.com/FourierSeries.html`.